



STOCHASTIC ANALYSIS OF OUTAGE PROBABILITY OF THE CASCADED RAYLEIGH-RICIAN FADING CHANNEL USING PADÉ APPROXIMATION METHOD

AUTHORS:

I. A. Ojedokun¹ and F. O. Aweda^{2*}

AFFILIATIONS:

¹Department of Electrical and Electronics Engineering, Bowen University, Iwo, Nigeria.

²Department of Physics, Bowen University, Iwo, Nigeria.

*CORRESPONDING AUTHOR:

Email: aweda.francis@bowen.edu.ng

ARTICLE HISTORY:

Received: 28 November, 2023.

Revised: 18 April, 2024.

Accepted: 27 April, 2024.

Published: 12 June, 2024.

KEYWORDS:

PDF, CDF, Outage Probability, Padé Approximation, Moment Generating Function.

ARTICLE INCLUDES:

Peer review

DATA AVAILABILITY:

On request from author(s)

EDITORS:

Chidozie Charles Nnaji

Patrick Akpan

FUNDING:

None

HOW TO CITE:

Ojedokun, I. A., and Aweda, F. O. "Stochastic Analysis of Outage Probability of the Cascaded Rayleigh-Rician Fading Channel using Padé Approximation Method", *Nigerian Journal of Technology*, 2024; 43(2), pp. 208 – 216; <https://doi.org/10.4314/njt.v43i2.2>

Abstract

The dominance of wireless communication (WC) is evident in all areas of life such as Information and Communication Technology (ICT), research, business, academia, etc. However, modelling analysis of WC has been a serious challenge when it involves diversity combining. Previous work has attempted to solve this problem using approximation techniques. These approximation techniques seem to be complex and may be difficult to interpret. The existing practice of using the Probability Density Function (PDF) to analyse multipath fading in a diversity-rich environment is ineffective to handle cascaded fading channels. The current work proposed the Padé Approximation (PA) technique to mitigate the problem. The PA was developed from the generated Moment Generating Function (MGF) by truncating the Taylor series to obtain a rational expression. The approximated rational expressions obtained were transformed into PDF, Cumulative Density Function (CDF) and Outage Probability (P_{out}). The results show that the P_{out} reduces as the threshold value increases. The numerical results also shows that the diversity techniques is effective in combating fading because as the number of paths increases, the P_{out} reduces. The P_{out} reduces by 17.56% at $L=4$ from 90.83% at $L=1$ when there is no diversity. PA is a useful approximation to analyse the behavior of cascaded Rayleigh-Rician channel.

1.0 INTRODUCTION

Due to the development of information technology, stochastic Wireless Communication Systems (WCS) have emerged as one of the key factors driving the global economy. Currently, speech, data, and internet signals are all sent and received primarily through WCS [1-3]. Wireless communication today makes it possible to provide multimedia services like sound, voice, video conferencing, data connections, and online remote instruction [4]. Fading distributions used in modelling wireless media propagation environments include but are not limited to Rayleigh, Rician, and Nakagami-m. Accurate knowledge of the environment's propagation characteristics is necessary for the design and planning of WCS [5]. Proper analysis of these fading distributions with Moment Generating Function (MGF), will help in studying the nature of the medium of propagation of the radio signal. The MGF is a helpful tool for streamlining diversity receiver modeling analysis. The last three decades of development have strengthened the case for the significance of this function [6-8].

The statistical analysis of the wireless communication channel can benefit greatly from this. Additionally, the Probability Density Function (PDF) and Cumulative Distribution Function (CDF) derivations are made simpler by MGF [9-11]. Approximation techniques can be used to truncate infinite series, such as the MGF series. However, WCS suffers from multipath propagation, which causes issues like fading and shadowing and consequently leading to fluctuation in the received signal quality [12]. Diversity combining methods have been employed in the past to address this multipath impairment, but they have largely relied on the Probability Density Function (PDF) for modelling purposes, which is inadequate to handle the two combined fading channels used to represent the cascaded fading channel [13]. Finding the PDF of the combined SNR per bit could be challenging where the fading distribution is of diverse sorts, according to [5]. In [14], a method of calculating the outage probability of block fading channels based on MGF was developed. The work developed analytic expressions that facilitate the determination of Outage Probability (P_{out}) using MGF in Nakagami-m and Rayleigh fading channels.

Reference [15] proposed a simple and accurate method to evaluate P_{out} of arbitrarily fading independent and identically distributed L-branch diversity receivers. This was based on Saddle Point Approximation (SPA) through the knowledge of MGF of the Signal to Noise Ratio (SNR) at the output of each diversity branch. This method required finding the MGF of the distribution, by which the Cumulative Generating Function (CGF) could be found. The authors were able to accurately model the estimation of the P_{out} for an arbitrary number of Maxima Ratio Combining (MRC) combined signals. The solution of the closed-form expression derived required, in general, solving a scalar non-linear equation whose solution is possible. The research was able to find the CDF from which the Outage Probability (P_{out}) was obtained. The outage analysis was carried out over a single Nakagami-m, Rice and Hoyt fading channels independently. The analytical expression obtained cannot handle the cascaded channel that the current work proposed.

[16] presented the analysis of the performance of the Free Space Optical (FSO) diversity system over the correlated Gamma-Gamma ($\Gamma\Gamma$) fading channel using the Padé Approximation (PA) method. The author identified the deficiency of the FSO line under clear weather conditions as atmospheric turbulence which is due to the homogeneities in the temperature and the

pressure of the atmosphere, resulting in variations of the air refractive index. The authors derived an infinite series representation for the MGF of the sum of arbitrarily correlated Gamma-Gamma Random Variable (RV). A closed-form approximate expression for the PDF of the sum of $\Gamma\Gamma$ RVs was obtained from the MGF. This was obtained with the aid of PA after which inverse Laplace Transform was used to obtain the PDF. The performance of the system was evaluated using some numerical methods to illustrate the accuracy of the methods. The work concluded that the MGF method is simple and accurate to analyze the performance of communication systems. This current research employed the method used in the paper to solve the problem of multipath fading in cascaded Rayleigh-Rician fading distribution for satellite communication. However, [17-19] uses meteorological data to work on communication and prediction of climate as regards radio waves.

1.1 Cascaded Channel Diversity Technique

The satellite channel involves both the terrestrial and upper atmosphere. It is a combination of multiple channels which has been known to be modelled as a double Rician channel. In [20] it was called the combination of two Rician channels but in [21], the authors argued that it is a combination of Rayleigh and Rician. This has been proposed by other authors. This cascaded channel could be used to model satellite communication channels. Therefore, adopting this in wireless communication means that, the moments of Rayleigh and Rician distributions can be cascaded and analysed using statistical parameters in a diversity-rich environment. Hence, the diversity combining techniques MRC and Equal Gain Combining (EGC) are adopted in this work to investigate the effectiveness of the PA techniques of approximation.

The weighted sum of MRC and EGC techniques are given by [22] in Equations (1) and (2) respectively,

$$r_M(t) = \sum_{l=1}^L w_l R_l(t) \quad (1)$$

$$r_E(t) = \left(\sum_{l=1}^L R_l(t) \right)^2 \quad (2)$$

Where, $r_M(t)$ is the received signal at the output of MRC diversity technique, $r_E(t)$ is the received signal at the output of EGC diversity technique, L is the number of diversity path, w_l is known as the weighted factor for each path in MRC, and $R_l(t)$ is the signal received at the input of the diversity techniques.

The received signal $r(t)$ at the output of the diversity combiner over a flat fading channel in the presence of noise is expressed as;

$$r(t) = a_s S(t) + N(t) \quad (3)$$



Where, a_c is the complex low pass channel response of the cascaded Channel, $S(t)$ is the transmitted signal, $N(t)$ is the Additive White Gaussian Noise (AWGN) with zero mean and variance N_o in each branch.

2.0 MATERIALS AND METHOD

2.1 Development of the MGF of the Channel

By employing, the work of [22-24] the MGF of the cascaded channel is derived using the equation expressed by [16] as;

$$M_{XY}(S) = M_{X+Y}(S) = E\{\beta^{S(x+y)}\} = E\{\beta^{Sx}\} * E\{\beta^{Sy}\} = M_X(S) * M_Y(S) \tag{4}$$

Where $M_{XY}(S)$ is the MGF of the combined XY variables and S is the Laplace variable, $E\{.\}$ Is the expected value.

In terms of the expected value ($E\{.\}$) definition of MGF ($M_{XY}(S)$), Equation (4) might be referred to as a sum of two fading channels or a product fading channel in real MGF terms which is technically referred. In this study, we referred to it as a cascaded Rayleigh-Rician fading channel. Reference [25] developed these MGFs of the cascaded Rayleigh-Rician fading channel utilizing the MGF of Rayleigh and Rician distributions presented in [26]. The following equations were developed for a multipath environment, where space diversity is employed; hence, L is the number of paths and k_l is the line of sight component of the Rician distribution. At L = 1, this means that there is only a single path for the signal and thus no diversity is applied. The following power series were generated using Equation (4) above.

At L = 1: EGC = MRC

$$M_{YEGC}(s) = M_{YMRC}(s) = \sum_{n=0}^{\infty} \frac{l^{2n}\Gamma^2(1+n)}{n!(k_l+1)^n} {}_1F_1(-n; 1; -k_l)Y^n \tag{5}$$

$k_l = 0$;

$$M_Y(s) = \sum_{n=0}^{\infty} \frac{\Gamma^2(1+n)}{n!} {}_1F_1(-n; 1; 0)Y^n \tag{6}$$

$$M_{YEGC}(s) = 1 + y + 2y^2 + 6y^3 + 24y^4 + 120y^5 + 720y^6 + 5.04e^3y^7 + 4.03e^4y^8 + 3.63e^5y^9 + 3.63e^6y^{10} + 3.99e^7y^{11} + 4.79e^8y^{12} + 6.23e^9y^{13} + 8.72e^{10}y^{14} + 1.31e^{12}y^{15} + 2.09e^{13}y^{16} + 3.56e^{14}y^{17} + 6.4e^{15}y^{18} + 1.22e^{17}y^{19} + 2.43e^{18}y^{20} ... \tag{7}$$

$k_l = 10$;

$$M_{YEGC}(s) = 1 + y + 1.17y^2 + 1.57y^3 + 2.33y^4 + 3.83y^5 + 6.82y^6 + 13.12y^7 + 27.07y^8 + 59.49y^9 + 138.72y^{10} + 341.78y^{11} + 886.61y^{12} + 2.41e^3y^{13} + 6.88e^3y^{14} + 2.05e^4y^{15} + 6.36e^4y^{16} + 2.05e^5y^{17} + 6.88e^5y^{18} + 2.39e^6y^{19} + 8.59e^6y^{20} ... \tag{8}$$

EGC At L = 4

$$M_{YEGC}(s) = \sum_{n=0}^{\infty} \frac{4^{2n}\Gamma^2(1+n)}{n!(k_l+1)^n} {}_1F_1(-n; 1; -k_l)Y^n \tag{9}$$

$k_l = 0$;

$$M_{YEGC}(s) = 1 + 16y + 512y^2 + 2.46e^3y^3 + 1.57e^6y^4 + 1.26e^8y^5 + 1.21e^{10}y^6 + 1.35e^{12}y^7 + 1.73e^{14}y^8 + 2.49e^{16}y^9 + 3.99e^{18}y^{10} + 7.02e^{20}y^{11} + 1.35e^{23}y^{12} + 2.8e^{25}y^{13} + 6.28e^{27}y^{14} + 1.51e^{30}y^{15} + 3.86e^{32}y^{16} + 1.05e^{35}y^{17} + 3.02e^{37}y^{18} + 9.19e^{39}y^{19} + 2.94e^{42}y^{20} ... \tag{10}$$

$k_l = 10$;

$$M_{YEGC}(s) = \sum_{n=0}^{\infty} \frac{4^{2n}\Gamma^2(1+n)}{n!(11)^n} {}_1F_1(-n; 1; -10)Y^n \tag{11a}$$

$$M_{YEGC}(s) = 1 + 16y + 300.43y^2 + 6.42e^3y^3 + 1.53e^5y^4 + 4.01e^6y^5 + 1.14e^8y^6 + 3.52e^9y^7 + 1.16e^{11}y^8 + 4.09e^{12}y^9 + 1.53e^{14}y^{10} + 6.02e^{15}y^{11} + 2.5e^{17}y^{12} + 1.09e^{19}y^{13} + 4.96e^{20}y^{14} + 2.36e^{22}y^{15} + 1.17e^{24}y^{16} + 6.06e^{25}y^{17} + 3.25e^{27}y^{18} + 1.8e^{29}y^{19} + 1.04e^{31}y^{20} ... \tag{11b}$$

MRC At L = 4

$$M_{YMRC}(s) = \left(\sum_{n=0}^{\infty} \frac{\Gamma^2(1+n)}{n!(k_l+1)^n} {}_1F_1(-n; 1; -k_l)Y^n \right)^4 \tag{12}$$

$k_l = 0$;

$$M_{YMRC}(s) = 1 + y^4 + 16y^8 + 1.3e^3y^{12} + 3.32e^5y^{16} + 2.07e^8y^{20} + 2.69e^{11}y^{24} + 6.45e^{14}y^{28} + 2.64e^{18}y^{32} + 1.73e^{22}y^{36} + 1.73e^{26}y^{40} + 2.54e^{30}y^{44} + 5.26e^{34}y^{48} + 1.5e^{39}y^{52} + 5.78e^{43}y^{56} + 2.92e^{48}y^{60} + 1.92e^{53}y^{64} + 1.6e^{58}y^{68} + 1.68e^{63}y^{72} + 2.18e^{68}y^{76} + 3.5e^{73}y^{80} ... \tag{13}$$

$k_l = 10$;

$$M_{YMRC}(s) = 1 + y^4 + 1.9y^8 + 6.03y^{12} + 29.72y^{16} + 214.19y^{20} + 2.16e^3y^{24} + 2e^4y^{28} + 5.37e^5y^{32} + 1.25e^7y^{36} + 3.7e^8y^{40} + 1.36e^{10}y^{44} + 6.18e^{11}y^{48} + 3.4e^{13}y^{52} + 2.24e^{15}y^{56} + 1.76e^{17}y^{60} + 1.63e^{19}y^{64} + 1.77e^{21}y^{68} + 2.23e^{23}y^{72} + 3.25e^{26}y^{76} + 5.43e^{27}y^{80} ... \tag{14}$$

2.2 A Review of Padé Approximation (PA) Method

WCS involves several approximation approaches as a result of meeting exceedingly complex infinite series. Gaussian Approximation (G_sA), Chernorf Bound Approximation (CBA), Gamma Approximation (GA), Padé Approximation (PA), and Saddle Point Approximation (SPA) are a few examples. The majority of the approximation methods given are straightforward in computing some of the performance measures in WCS, while some are poor in dealing with other performance metrics, implying that a perfect approximation may be difficult to find. Furthermore, some of these approximations are known to be quite complex, involving numerous complex integrals. PA is a rational function approximation of an infinite power series that may not be useful in further computation in its natural form. A power series, such as Equation (4) which results in Equations (5) to (14), is in the form of $f(z)$, and is expressed in Equation (15) where the variable Z is the set of complex numbers,

$$f(z) = \sum_{n=0}^{\infty} D_n Z^n, \tag{15}$$

Where D_n is the set of real numbers.



To accurately describe the limiting behaviour of the power series in Equation (15), a compact rational approximation is preferred. To facilitate further computation, this equation is approximated in a rational form in this study. The series is transformed into the one-point PA of order $\left(\frac{A}{B}\right)$, where A is the highest power of the polynomial in the numerator and B is that of the denominator, which is $P_{\frac{A}{B}}(Z)$ and given by ([10], [4], [27-28]) as;

$$P_{\frac{A}{B}}(x) = \frac{\sum_{i=0}^A a_i x^i}{\sum_{j=0}^B b_j x^j} = \sum_{n=0}^N D_n x^n \tag{16}$$

The coefficient a_i and b_j are real coefficients defined such that;

$$\sum_{n=0}^N D_n x^n = \frac{\sum_{i=0}^A a_i x^i}{\sum_{j=0}^B b_j x^j} = \sum_{n=0}^{A+B} H_n x^n + R(x^{A+B+1}) \tag{17}$$

$R(x^{A+B+1})$ stands for terms of order greater than A+B and represents the remaining terms after PA has truncated the Equation (16). The moment matching method is used to determine the coefficients a_i and b_j . This is accomplished by matching the power series coefficients on both sides of the Equation (17). Without losing generality, Equation (16) forms a set of equations obtained as follows, from Equation (17) and neglecting the remainder, $R(x^{A+B+1})$, cross multiplication yields;

$$\sum_{i=0}^A a_i x^i = \sum_{j=0}^B b_j x^j \times \sum_{n=0}^{A+B} H_n x^n \tag{18}$$

The product of Equation (18) is obtained as

$$\sum_{j=1}^B b_j h_{A-j+l} = 0 \quad 0 \leq l \leq B \tag{19}$$

A system of B linear equations for the B unknown denominator coefficients is formed by the set of equations that follow from Equation (19) above. Therefore, the matrix form of this set of equations can be stated as follows;

$$Hb = -h \tag{20}$$

Where, $b = (b_B \dots b_k \dots b_1)^T$, $H = (h_{A+1} \dots h_{A+k+1} \dots h_{A+B})^T$

$$H = \begin{bmatrix} h_{A-B+1} & h_{A-B+2} & \dots & h_A \\ \vdots & \vdots & \vdots & \vdots \\ h_{A-B+k} & h_{A-B+k+1} & \dots & h_{A+k-1} \\ \vdots & \vdots & \vdots & \vdots \\ h_A & h_{A+1} & \dots & h_{A+B-1} \end{bmatrix} \tag{21}$$

$$\begin{bmatrix} h_{A-B+1} & h_{A-B+2} & \dots & h_A \\ \vdots & \vdots & \vdots & \vdots \\ h_{A-B+k} & h_{A-B+k+1} & \dots & h_{A+k-1} \\ \vdots & \vdots & \vdots & \vdots \\ h_A & h_{A+1} & \dots & h_{A+B-1} \end{bmatrix} \begin{bmatrix} b_B \\ \vdots \\ b_k \\ \vdots \\ b_1 \end{bmatrix} = - \begin{bmatrix} h_{A+1} \\ \vdots \\ h_{A+k+1} \\ \vdots \\ h_{A+B} \end{bmatrix} \tag{22}$$

The $(.)^T$ is the transpose operator of a matrix. The coefficients b_i can be determined after solving the matrix equation in Equations (19) and (22). Hence, coefficients a_i are calculated by backward substitution from;

$$a_i = h_i + \sum_{t=1}^{\min(B,i)} b_t h_{i-t} = 0; \quad 0 \leq i \leq A \tag{23}$$

The selection of ‘A’ and ‘B’ was not made at random. Given what is known about determinants, |H|, the determinant of the variable ‘H’ must be zero for this equation to have a unique solution. Matrix ‘H’ in PA decisions is frequently a Hankel matrix. The determinant of the Hankel matrix ‘H’ must exist otherwise the matrix is rank deficient. The value of ‘B’ above which the matrix ‘H’ becomes rank deficient was determined by [10] using the rank order plot. If A is one less than B, the convergence of the PA can be assured ([27], [29-30]).

2.3 Approximated PDF and CDF from PA

The PDF approach of evaluating WCS performance required the existence of the PDF. The PDF of the cascaded fading channel is unknown in this investigation. As a result, the PDF over the combined channel was calculated using the MGF technique with PA. PA is only used in the direct approximation of the developed MGF with known expansion coefficients. The PDF of the combined fading distributions from moments was estimated using the PA. The Residue Inversion Formula (RIF) is used to calculate this PDF from MGF, Equations (5) to (14) are resolved to a partial fraction of the form,

$$P_{\frac{A}{B}}(x) = \frac{\sum_{i=0}^A a_i x^i}{\sum_{j=0}^B b_j x^j} = \sum_{n=0}^{A+B} H_n x^n = \sum_{i=1}^B \frac{\lambda_i}{x+P_i} \tag{24}$$

Since $b_0 = 1$, Equation (9) is

$$P_{\frac{A}{B}}(x) = \frac{\sum_{i=0}^A a_i x^i}{1 + \sum_{j=1}^B b_j x^j} = \sum_{i=1}^B \frac{\lambda_i}{x+P_i} \tag{25}$$

The PA is resolved to sums of partial fractions because the MGF of any distribution is the Laplace Transform (LT) of the distribution's expected value. The partial fraction's residues, λ_i and poles, P_i were then deduced from Equations (25) to determine the PDF and CDF of the cascaded fading channel using Equations (26) and (27) as given by [16].

$$PDF = f(x) = \sum_{i=1}^B \lambda_i e^{-P_i x} \tag{26}$$

$$CDF = F(x) = C_\gamma(y) = 1 - \sum_{i=1}^B \frac{\lambda_i}{P_i} e^{-P_i x} \tag{27}$$

Where λ_i and P_i are residues and poles obtained from partial fraction decomposition of PA respectively, using the RIF, this is done by finding the partial fraction expansion of the PA. The following equations were generated using the MATLAB package from Equations (25), (26) and (27). Figure 1 shows the step-by-step procedures to obtain PA, PDFs, and CDFs.

3.0 RESULTS AND DISCUSSION

3.1 Results of Developed PA, PDF, and CDF Expression

In this study all PAs $(R(y))$, PDFs $(f(y))$, and CDFs $(C_\gamma(y))$ were obtained respectively, from equations (25), (26) and (27); using Equations (5) to (14).



Equations (28) to (39) were consequently, obtained. When $L = 1$, EGC = MRC, this implies that there is no diversity. Therefore,

$$K = 0 \quad (y) = \frac{1-24y+177y^2-444y^3+274y^4}{1-25y+200y^2-600y^3+600y^4-120y^5} \quad (28)$$

$$K = 10 \quad R(y) = \frac{1-6.63y+14.51y^2-11.91y^3+2.87y^4}{1-7.63y+20.97y^2-25.49y^3+13.38y^4-2.34y^5} \quad (29)$$

The PDF derived from the PA based on Equation (26) are as follows:

When $L = 1, K = 0$
 $f(y) = 0.004e^{-7.09y} + 0.08e^{-3.6y} + 0.4e^{-1.41y} + 0.52e^{-0.26y}$ (30)

$L = 1, K = 10$
 $f(y) = -0.004e^{-3.05y} + 0.06e^{-2.1y} + 0.34e^{-1.35y} + 0.5e^{-0.79y} + 0.11e^{-0.35y}$ (31)

3.1.1 Derived EGC Padé approximation

$K = 0$, and $L = 4$
 $R(y) = \frac{1-384y+4.53e^4y^2-1.82e^6y^3+1.8e^7y^4}{1-400y+5.21e^4y^2-2.46e^6y^3+3.93e^7y^4-1.26e^7y^5}$ (32)

$K = 10$ and $L = 4$
 $R(y) = \frac{1-106.08y+3.71e^3y^2-4.88e^4y^3+1.88e^5y^4}{1-122.08y+5.37e^3y^2-1.04e^5y^3+8.77e^5y^4-2.45e^6y^5}$ (33)

3.1.2 Derived PDF of EGC

$L = 4, K = 0$
 $f(y) = -0.0003e^{-202.48y} + 0.002e^{-112.69y} + 0.084e^{-58.17y} + 0.389e^{-22.44y} + 0.52e^{-4.23y}$ (34)

$L = 4, K = 10$
 $f(y) = -0.16e^{-46.44y} + 0.35e^{-38.33y} + (0.35 + 1.9j)e^{-(16+0.45j)y} + (0.35 - 1.9j)e^{-(16-0.45j)y} + 0.11e^{-5.4y} = -0.16e^{-46.44y} + 0.35e^{-38.33y} + 0.7e^{-16y} \cos 0.45y + 3.8e^{-16y} \sin 0.45y + 0.11e^{-5.4y}$ (35)

3.1.3 Derived MRC Padé approximation

$K = 0$, and $L = 4$ for P_4^3 because Hankel matrix rank deficient at $n > 8$

$$R(y) = \frac{1-3.74e^3y+1.88e^6y^2-9.06e^7y^3}{1-3.74e^3y+1.89e^6y^2-9.24e^7y^3+6.67e^7y^4} \quad (36)$$

$K = 10$ and $L = 4$
 $R(y) = \frac{1-59.04y+940.37y^2-4.53e^3y^3+4.93e^5y^4}{1-60.04y+998.51y^2-5.42e^3y^3+8.79e^3y^4-2.97e^3y^5}$ (37)

3.1.4 Derived PDF of MRC

$L = 4, K = 0$ Hankel matrix rank deficient at the order of PA greater than P_4^3

$$f(y) = -0.0012e^{-3149.2y} + 0.0055e^{-536.2y} + 0.0003e^{-53.9y} + 0.9954e^{-0.7y}$$
 (38)

$L = 4, K = 10$
 $f(y) = 0.584e^{-36.66y} - 13.23e^{-14.98y} + 80.99e^{-5.95y} - 177.63e^{-2y} + 110.28e^{-0.46y}$ (39)

3.2 Developed Outage Probability

The outage probability (P_{out}), measures the likely probability of signal outage at a normalized threshold value irrespective of the modulation technique in use. The CDF, C_y is the outage probability given in Equations (40) to (45) below:

CDF (No Diversity)

$L = 1, K = 0$
 $C_y(y) = 1 - 0.00005e^{-7.09y} - 0.021e^{-3.6y} - 0.282e^{-1.41y} - 1.98e^{-0.26y}$ (40)

$L = 1, K = 10$
 $C_y(y) = 1 + 0.0014e^{-3.05y} - 0.031e^{-2.1y} - 0.249e^{-1.35y} - 0.63e^{-0.79y} - 0.318e^{-0.35y}$ (41)

3.2.1 Derived CDF of EGC from Equation (27)

$L = 4, K = 0$
 $C_y(y) = 1 + 1.5 \times 10^{-6}e^{-202.48y} - 1.6 \times 10^{-5}e^{-112.69y} - 1.5 \times 10^{-3}e^{-58.17y} - 0.0173e^{-22.44y} - 0.124e^{-4.23y}$ (42)

$L = 4, K = 10$
 $C_y(y) = 1 + 0.004e^{-46.44y} - 0.009e^{-38.33y} - (0.02 + 0.12j)e^{-(16+0.45j)y} - (0.02 + 0.12j)e^{-(16-0.45j)y} - 0.021e^{-5.4y} = 1 + 0.004e^{-46.44y} - 0.009e^{-38.33y} - 0.04e^{-16y} \cos 0.45y - 0.24e^{-16y} \sin 0.45y - 0.021e^{-5.4y}$ (43)

3.2.2 Derived CDF of MRC

$L = 4, K = 0$ Hankel matrix rank deficient at the order of PA greater than P_4^3

$$C_y(y) = 1 + 3.8 \times 10^{-7}e^{-3149.2y} - 1.03 \times 10^{-5}e^{-536.2y} - 5.6 \times 10^{-6}e^{-53.9y} - 1.4 \times 10^{-3}e^{-0.7y}$$
 (44)

$L = 4, K = 10$
 $C_y(y) = 1 - 0.016e^{-36.66y} + 0.883e^{-14.98y} - 13.61e^{-5.95y} + 88.98e^{-2y} - 242.2e^{-0.46y}$ (45)

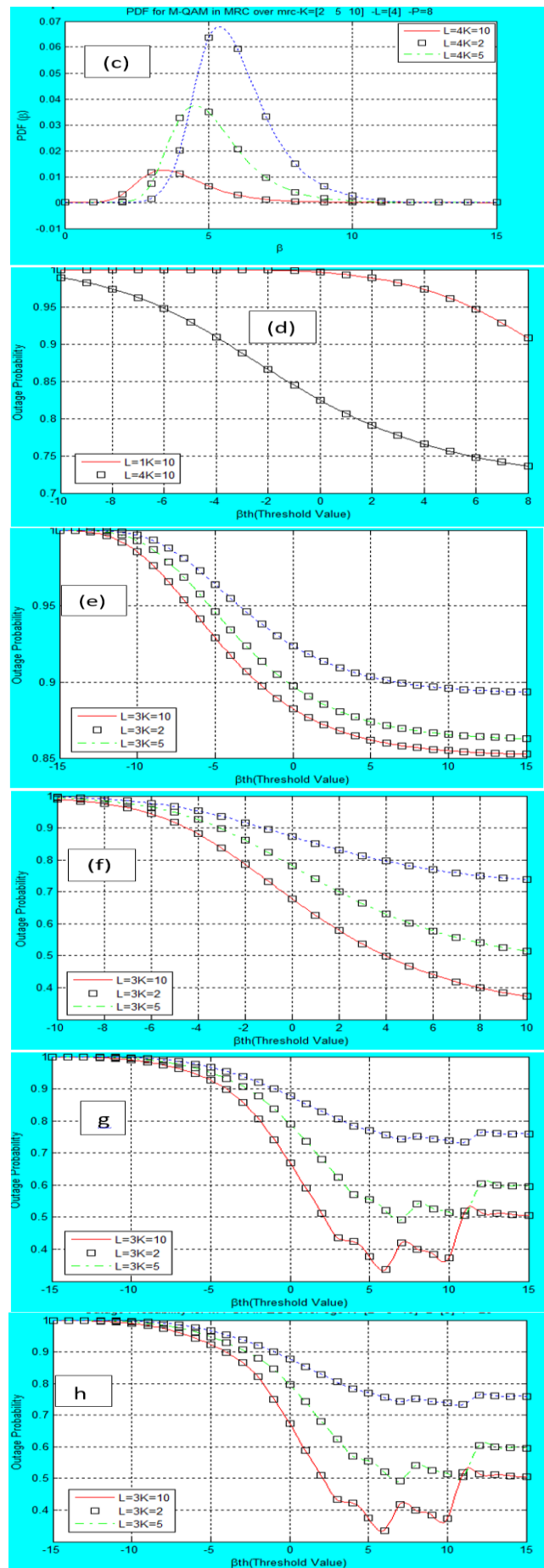
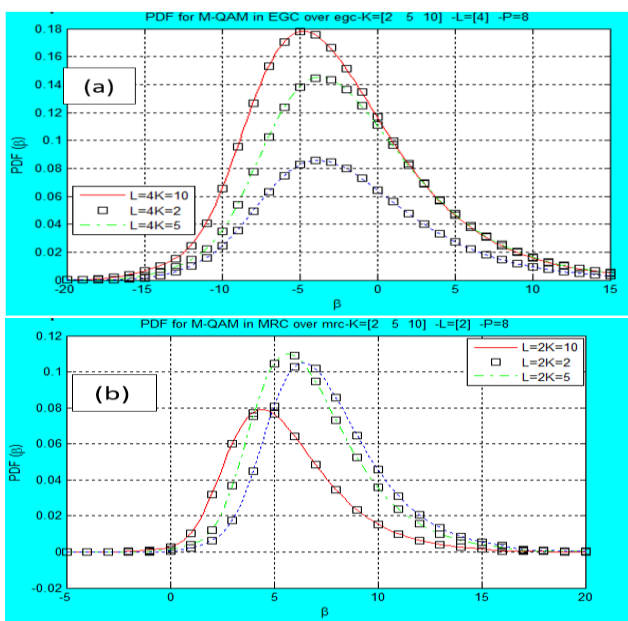
3.3 Discussion

The CDF in statistical communication is the outage probability, the results of which have been extensively discussed earlier. The results are as presented in Figures 1(a to j), Figures 1(a to c) show the PDF of EGC at $L = 4$, the PDF of MRC at $L = 2$ and $L = 4$ in the cascaded Rayleigh and Rician fading channel respectively at $K = 2, 5$ and 10 dB. Figure 1(d) shows the P_{out} for two different values of L ($L = 1, 4$) at $K = 10$ at $L = 1$, (when there is no diversity), and $L = 4$ which is when diversity was introduced respectively. Figure 1(d) shows that when there is no diversity ($L = 1$) the P_{out} at -4 dB threshold was 99.99% and at $L = 4$ the P_{out} was 90.72% while at a threshold value of 7dB, the P_{out} were 90.83% and 73.56% for $L = 1$ and $L = 4$ respectively. In Figure 1(e), the results depict the effects of increasing the of K , with the number of paths, $L = 3$, there is an improvement as the P_{out} at 5 dB threshold value and $K = 10, 5, 2$, the outage probability is 46.9%, 60.12% and 78.3% respectively. In Figures 1(d and e) respectively at the 10 dB threshold, the value P_{out} obtained was 65.44%, 76.19% and 86.47%; 37.26%, 51.39% and 73.83%.

In Figure 1(f) at a PA order 5, (P_5^2), at a 15 dB threshold value, the P_{out} obtained was 85.24%, 86.27% and 89.33% for $K = 10, 5, 2$ respectively. Figure 1(g) shows the result at PA of order P_8^7 for 10 dB, the P_{out}

were 37.19%, 51.5% and 73.84%, whereas at 15 dB the P_{out} were 50.17%, 59.51 and 75.84% respectively. A similar result is shown in Figure 1(j) for a PA of order, P_{10}^9 . The results above were obtained over EGC; similar results were also obtained over MRC. Figures (i and j) compare the results at P_5^4 and P_{10}^9 respectively for P_{out} of $K = 5, 10$. The P_{out} at a threshold value of 5 dB and $L = 2$ in Figure 1(j) were 91.5% and 87.35% respectively but at 12 dB the P_{out} were observed to be 67.67% and 58.34% respectively. In Figure 1(a), the PDF with the highest altitude was the PDF of $K = 10$ while the lowest was at $K = 2$. The PDF is a useful function in determining the Bit Error Rate (BER). This is not unconnected to the fact that at weak LOS the BER is always high and at strong LOS the BER is expected to be low. Figures 1(b) and 1(c) show a similar result over MRC.

The results in Figures 1(d and e) reveal that as the threshold value increases the P_{out} reduces, also as the diversity order, and a number of paths, increase, the P_{out} becomes very low, but on the contrary, as the LOS reduces the P_{out} increases. The weaker the LOS, the more likely an outage should be expected. This is a normal occurrence in practical situations. Figures 1(f-h) investigate the effects of PA order on the outage probability performance. The figures show that at higher order PA, the model is unstable at higher SNR, these results show that at higher order PA, the PA becomes unstable, unlike the lower order. A similar result is shown in Figure 1(h) for a PA of order, P_{10}^9 , the higher order PA is therefore, erratic, unstable, and inconsistent at higher SNR, which makes it undesirable.



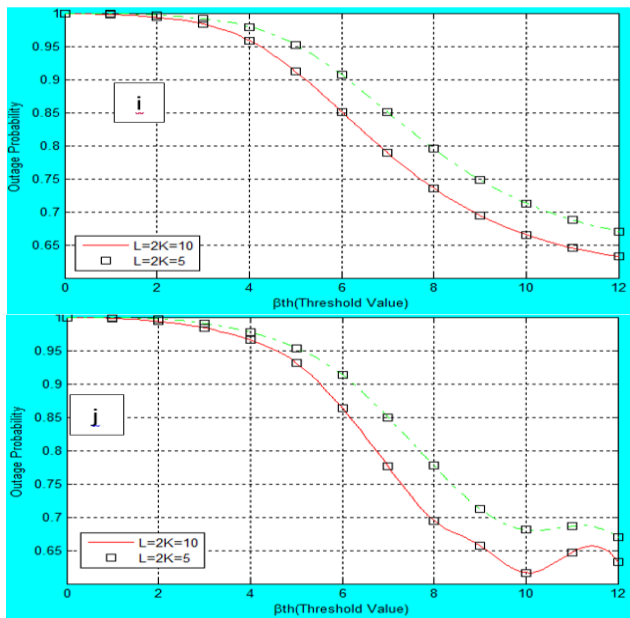


Figure 1: PDF of cascaded Fading channel versus SNR

Figure 1(j) was obtained at a higher PA of order P_{10}^9 , consequently, its fluctuation at high threshold values (β_{th}) of SNR. In comparison to Figure 1(i) which is for a PA of order P_5^4 , a similar result was obtained at 5 dB and 12 dB, but there is fluctuation at higher values of SNR. This comparison emphasizes the unstable behaviour of higher-order PA in this research; this has earlier been reported by [22]. Figure 1(a) is the PDF of cascaded Fading channel versus SNR with $L = 4$ over EGC at different LOS, while Figure 1(b) is the PDF of cascaded Fading channel versus SNR with $L = 2$ over MRC at different LOS more so, Figure 1(c) PDF of cascaded Fading channel versus SNR with $L = 4$ over MRC at different LOS. Figure 1(d) is known as Outage Probability versus threshold value (β_{th}) of cascaded Fading channel with $L = 1$ (no diversity) and $L = 4$ with diversity $K = 10$. Figure 1(e) represent the Outage Probability versus threshold value (β_{th}) of cascaded Fading channel with $L = 3$ Over EGC at different LOS ($K = 2, 5, 10$).

Figure 1(f) is the Outage Probability versus threshold value (β_{th}) of cascaded Fading channel with $L = 3$ over EGC at different LOS ($K = 2, 5, 10$) and PA of order P_5^2 . Figure 1(g) is the Outage Probability versus threshold value (β_{th}) of cascaded Fading channel with $L = 3$ over EGC at different LOS ($K = 2, 5, 10$) and PA of order P_5^7 . Figure 1(h) is the Outage Probability versus threshold value (β_{th}) of cascaded Fading channel with $L = 3$ over EGC at different LOS ($K = 2, 5, 10$) and PA of order P_{10}^9 . Figure 1(i) Outage Probability versus threshold value (β_{th}) of cascaded

Fading channel with $L = 2$ Over MRC at different LOS and PA of order P_5^4 . Figure 1(j) is the Outage Probability versus threshold value (β_{th}) of cascaded Fading channel $L = 2$ Over MRC at different LOS and PA of order P_{10}^9 .

4.0 CONCLUSION

This work has been able to analyse outage probability in a cascaded Rayleigh-Rician fading channel. The PDF of the cascaded channel was obtained for two diversity combining EGC and MRC. Consequently, an investigation of the effectiveness of PA in stochastic analysis of the fading channel was carried out. The higher-order PA is found to be unstable, and inconsistent at higher SNR.

REFERENCES

- [1] Jochen, S. "Mobile Communications", *Pearson Education Ltd.*, India. pp. 513. 2006.
- [2] Stallings, W. "Wireless Communications and Networks", *Third Indian Reprint, Pearson Education Ltd.*, India, pp. 763. 2003.
- [3] Stuber, G. L. "Principles of Mobile Communication", *Kluwer Academic Publishers New York, USA*, pp. 771. 2002.
- [4] Karagiannidis, G. K., Sagias N. C. and Zogas D. A. "Error Analysis of M-QAM with Equal Gain Combining Diversity over Generalized Fading Channels", *IEEE Transactions on wireless communications*, 152(1):69-74. 2005.
- [5] Iskander, I. A. and Yun, Z. "Propagation Predictions Models for Wireless Communication System", *IEEE Transactions on Microwave Theory and Techniques*, 50(3):662-673. 2002.
- [6] Abolade, R. O., Adeyemo, Z. K., Ojedokun, I. A. and Ojo, S. I. "Moment Generating Function Analysis of Spatial Diversity Combining in a Composite Fading Channel", *International Journal of Innovation, Technology, and Computing Science IJITCS-V11-N10*. 2019
- [7] Yilmaz, F. and Alouini, M. "Unified MGF – Based Capacity Analysis of Diversity Combiners over Generalized Fading Channels", *IEEE Transactions on Communications*, 10(20):1-26. 2010.
- [8] Zogas, D. A., Karagiannidis G. K. and Kotsopoulous, S. A. "Equal Gain Combining over Nakagami-n(Rice) and Nakagami-q (Hoyt) Generalized fading Channels", *IEEE Transactions on wireless communications*, 4(2):374-379. 2005.
- [9] Amindavar, H. "Application of Padé Approximation in Signal Analysis",



- Unpublished PhD Thesis*, University of Washington, pp. 187. 1991.
- [10] Amindavar H. and Ritcey J.A. Padé Approximation of Probability Density Functions, *IEEE Transactions on Aerospace and Electron System*, 30(2):416-424. 1994.
- [11] Abolade, R. O., Adeyemo, Z. K., Ojedokun, I. A. and Ojo, S. I. "Moment Generating Function Analysis of Spatial Diversity Combining in a Composite Fading Channel", *International Journal of Innovation, Technology, and Computing Science*, IJITCS-V11-N10. 2019.
- [12] Kolosov V. V., Kulikov V. A., and Polnau E. "Dependence of Laser Radiation Power on the Scintillation Index and the Size of a Receiver Aperture", *Optical Express*, Vol. 30, Issue 2, pp. 3016-3034. 2022
- [13] Kupferman, J and Arnon S. "Communication System Performance at mm and THz as a function of PDF Model", *Sensors*, 22(16), 6269 pp. 1-12, 2022.
- [14] Yilmaz, A. O. "Calculating Outage Probability of Block Fading Channels Based on Moment Generating Function", *IEEE Transactions on Communications*, 59(11):2945-2950. 2011.
- [15] Jabi, M., Szczecinski, L. and Benjillali, M. "Accurate Outage Approximations of MRC Receivers in Arbitrarily Fading Channel", *IEEE Communication Letters* 16(18):789-792. 2012.
- [16] Yang, G., Khalighi, M.A., Ghassemlooy, Z. and Bourennane, "Performance Analysis of Space Diversity FSO Systems over the Correlated Gamma-Gamma Fading Channel Using Padé Approximation Method", *IET Communication*, 8(13):2246-2255. 2014.
- [17] Adebayo, S., Aweda, F. O., Ojedokun, I. A., Olapade, O. T. "Refractive Index Perception and Prediction of Radio Wave through Recursive Neural Networks using Meteorological Data Parameters", *International Journal of Engineering, Transactions A: Basics* 35(4): 810-818. 2022.
- [18] Aweda, F. O., Akinpelu, J. A., Samson, T. K., Sanni, M., Olatinwo, B. S. "Modeling and Forecasting Selected Meteorological Parameters for the Environmental Awareness in Sub-Sahel West Africa Stations", *Journal of the Nigerian Society of Physical Sciences*, 4(3):1-13. 2022.
- [19] Aweda, F. O., Olufemi, S. J., Agbolade, J. O. "Meteorological Parameters Study and Forecasting Temperature Across Selected Stations in Sub-Sahara Africa Using MERRA-2 Data". *Nigerian Journal of Technological Development(NJTD)*. 19(1): 80 – 91. 2022.
- [20] Pornchai, S., Wanaree, W. and Sawasd, T. "Performance of M-PSK in Mobile Satellite Communication over Combined Ionosphere Scintillation and Flat Fading Channels with MRC Diversity", *IEEE Transactions on Wireless Communications*, 8(7):3360-3364. 2009
- [21] Adeyemo, Z. K., Ojedokun, I. A. and Akande, D. O. "Symbol Error Rate Analysis of M-QAM with Equal Gain combining over a Mobile Satellite Channel", *International Journal of Electrical and Computer Engineering* 3(6):849-856. 2013.
- [22] Zhang, Y., Wen, J., Yang, G., He, Z. and Wang, J. "Path loss prediction based on machine learning: Principle, method, and data expansion", *Applied Sciences*, Vol. 9, No. 9, 1-18, 1908. 2019.
- [23] Afonja, B., Olubusoye, O. E., Ossai, E. and Arinola, J. "Introductory Statistics: A Learner's Motivated Approach", Evans Brothers Limited, Ibadan, Nigeria. pp. 545. 2014.
- [24] Agbolade, J. O., Ojedokun, I. A., Fabunmi, E. Y., Adebayo, A. K. and Bamikefa, I. A. "Modelling Efficacy of Probability Density Functions (PDF) in Wireless Communication", *International Journal of Sciences, Engineering & Environmental Technology (IJOSEET)*, 7(9): 80-90. 2022.
- [25] Ojedokun, I. A. "Development of Approx. Moment Generating Function Based Models for Spatial Diversity Combining Over Composite Fading Channel", *Unpublished PhD Dissertation*, Ladoke Akintola University of Technology, Ogbomoso, Nigeria, pp. 119. 2019.
- [26] Simon, M. K. and Alouini, M. S. "Digital Commun. over fading channels", *John Wiley and Sons*. Inc. Hoboken, New Jersey, pp. 937. 2005.
- [27] Ismail, M. H. and Matalgah, M. M. "On the Use of Padé Approximation for Performance Evaluation of Maximal Ratio Combining Diversity Over Weibull Fading Channels" *EURASIP Journal on Wireless Communications and Networking*, 2006(3):62-68. 2006.
- [28] Suetin, S. P. "Padé Approximants and Efficient Analytical Continuation of a Power Series", *Russian Mathematical Surveys*, 57(1):43-141. 2002.
- [29] Baker, G. A. and Graves-Morris, P. "Padé Approximants, Cambridge University Press", United Kingdom, pp. 386. 1996.



- [30] Jay, E., Ovarlez, J. P. and Duvaut, P. “New Method of Radar Performances Analysis”, *Signal Processing*, 80(12):2527-2540. 2000.

